ECCOMAS Congress 2016
VII European Congress on Computational Methods in Applied Sciences and Engineering
M. Papadrakakis, V. Papadopoulos, G. Stefanou, V. Plevris (eds.)
Crete Island, Greece, 5–10 June 2016

DEVELOPMENT OF CONFINED VISCOPLASTIC FLOWS WITH HETEROGENEOUS WALL SLIP

Pandelitsa Panaseti[1], Maria Philippou[1], Zacharias Kountouriotis[1], Georgios Georgiou[1]

[1] Department of Mathematics and Statistics, University of Cyprus
PO Box 20537, 1678 Nicosia, Cyprus
{panaseti.pandelitsa, filippou.maria, kountouriotis.zacharias, georgios}@ucy.ac.cy

Keywords: Plane Poiseuille Flow, Bingham plastic, Wall Slip, Navier Slip, Flow Development, Finite Elements.

Abstract. *The steady, pressure-driven flow of a Herschel-Bulkley fluid in a channel is considered assuming that slip occurs on one wall only due to slip heterogeneities. Hence, the velocity profile is allowed to be asymmetric. The fully-developed solutions are derived and the different flow regimes are identified. The development of the flow is investigated numerically using the Papanastasiou regularization for the constitutive equation, a power-law slip equation, and finite element simulations. The combined effects of slip and the Bingham number are discussed.*

.

1 INTRODUCTION

Wall slip is important in many industrial applications, such as the extrusion of complex fluids, ink jet processes, oil migration in porous media, and in microfluidics. Viscoplastic or yield stress materials, such as polymeric solutions, suspensions, and gels, are known to exhibit wall slip [1-3]. While wall slip with polymer melts is observed at large rates of strains, it appears within a range of rather small strains in the case of pasty materials [4]. Based on the analysis of apparent slip flows of Herschel-Bulkley fluids in various geometries, Kalyon [5] proposed a power-law slip equation, relating the wall shear stress, τ_w, to the slip (or sliding) velocity, u_w, defined as the relative velocity of the fluid with respect to that of the wall,

$$\tau_w = \beta u_w^s \tag{1}$$

where s is the exponent, and β is the slip coefficient. The latter incorporates the effects of all other factors affecting slip, such as the temperature, the normal stress, the molecular parameters, and the properties of the fluid/wall interface [4]. Setting s=1 in Eq. (1) leads to the classical Navier slip condition [6]

$$\tau_w = \beta u_w \tag{2}$$

in which case β is related to the so-called slip (or extrapolation) length b, i.e. $\beta \equiv \mu / b$, where μ denotes the viscosity. The no-slip and full-slip limiting cases are recovered when $\beta \to \infty$ and $\beta = 0$, respectively.

The present work is motivated by the recent findings of Vayssade et al. [7] who imaged the motion of well characterized softy glassy suspensions in microchannels whose walls impose different slip velocities. These materials exhibit yield stress and are modeled as Herschel-Bulkley fluids. The Herschel-Bulkley constitutive equation, which involves three material parameters, the yield stress τ_0, the consistency index k, and the power-law exponent, n. The tensor form of the model is as follows:

$$\begin{cases} \dot{\boldsymbol{\gamma}} = \mathbf{0}, & \tau \le \tau_0 \\ \boldsymbol{\tau} = \left(\dfrac{\tau_0}{\dot{\gamma}} + \mathrm{k}\dot{\gamma}^{\mathrm{n}-1} \right) \dot{\boldsymbol{\gamma}}, & \tau > \tau_0 \end{cases} \tag{3}$$

where $\boldsymbol{\tau}$ is the viscous stress tensor, $\dot{\boldsymbol{\gamma}} \equiv \nabla \mathbf{u} + (\nabla \mathbf{u})^T$ is the rate of strain tensor, $\mathbf{u}$ is the velocity vector, and the superscript T denotes the transpose. The magnitudes of $\dot{\boldsymbol{\gamma}}$ and $\boldsymbol{\tau}$, denoted respectively by $\dot{\gamma}$ and τ, are defined by $\dot{\gamma} \equiv \sqrt{\dot{\boldsymbol{\gamma}} : \dot{\boldsymbol{\gamma}} / 2}$ and $\tau \equiv \sqrt{\boldsymbol{\tau} : \boldsymbol{\tau} / 2}$, where the symbol II stands for the second invariant of a tensor.

The experiments showed that as the channel height decreases the flow ceases to be symmetric and slip heterogeneities effects become important [7]. Some of the experimental velocity profiles are characterized by overshoots similar to those encountered in entry flows. We thus revisited the classical flow development problem of a Bingham plastic with asymmetric wall slip, i.e. with different Navier slip conditions at the two walls. If slip occurs along both walls and slip at the upper wall is stronger, there are three flow regimes depending on the pressure gradient, as illustrated in Fig. 1. Below a certain critical value G_1 (Regime I) the fluid simply slides and the velocity is plug. Above G_1 (Regime II), the fluid yields only near the lower plate and the unyielded region extends up to the upper wall. Finally, above a second critical pressure gradient G_2 (Regime III), the fluid yields near both the walls and the velocity profile is asymmetric with a plug core. For simplicity, in the present work we assume that along the lower wall there is no slip, as in Fig. 2. In such a case only Regimes II and III are relevant.

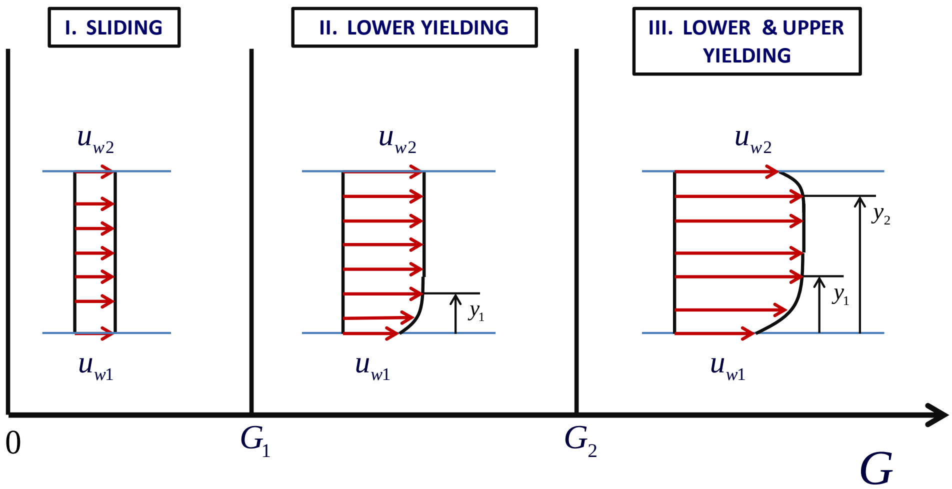

Figure 1: Different flow regimes in the case of plane viscoplastic Poiseuille flow with asymmetric slip.

In the literature, the development length is usually defined as the length required for the maximum velocity to attain 99% of its fully-developed value scaled either by the pipe diameter or the channel width [9]. This definition implies that maximum velocity develops more slowly than its counterparts at any other vertical distance which may not be the case in all geometries and for all fluids, especially viscoplastic ones which are characterized by a maximum flat velocity. For the asymmetric flow under study, we define as development length the smallest length at which the velocity at any vertical distance differs from its fully developed value by 0.01%. Hence, the velocity is required to attain either 99% or 1.01% of its fully developed value, depending on whether the latter is greater or less than unity.

The governing equations are presented in Section 2 where the solutions corresponding to fully-developed flow are also derived and the various flow regimes are identified. In Section 3, the numerical method is briefly presented and preliminary results are discussed. Finally, the conclusions are summarized in Section 4.

2 GOVERNING EQUATIONS

The governing equations are de-dimensionalized scaling lengths by the gap height H of the channel, the velocity vector by the uniform inlet velocity U, and the pressure and the stress tensor components by kU^n/H^n. If we denote de-dimensionalized variables with stars, then the continuity and momentum equations for steady incompressible flow with zero gravity read:

$$\nabla^* \cdot \mathbf{u}^* = 0 \tag{4}$$

and

$$Re\,\mathbf{u}^* \cdot \nabla^* \mathbf{u}^* = -\nabla^* p + \nabla^* \cdot \boldsymbol{\tau}^* \tag{5}$$

respectively, where $Re \equiv \rho U^{2-n} H^n / k$ is the Reynolds number, ρ being the constant density of the material.

The standard finite element method and the Pananastasiou regularization [8] are used in order to solve the flow numerically. The dimensionless form of the Papanastasiou-regularized constitutive equation is written as follows:

$$\boldsymbol{\tau}^* = \left[Bn \frac{1-\exp(-M\dot{\gamma}^*)}{\dot{\gamma}^*} + \dot{\gamma}^{*n-1} \right] \dot{\boldsymbol{\gamma}}^* \tag{6}$$

where $Bn \equiv \tau_0 H^n / (kU^n)$ is the Bingham number and $M \equiv mU / H$ is the dimensionless growth exponent, which has to be sufficiently high so that the flow of the ideal discontinuous Herschel-Bulkley fluid is approximated satisfactorily [8].

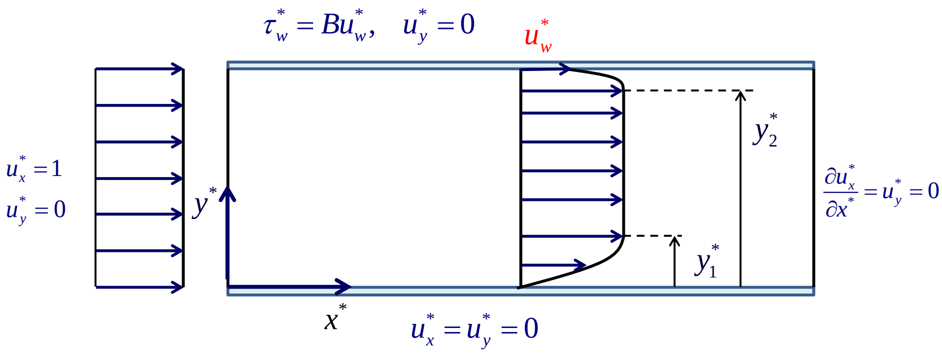

Figure 2: Geometry and boundary conditions of the flow development of a Bingham plastic in a channel with slip along the upper wall.

The geometry and the boundary conditions of the flow are illustrated in Fig. 2. At the inlet plane, the velocity component in the direction of the flow is uniform ($u_x^* = 1$) and the transversal one vanishes. At the lower wall there is no slip and no penetration so that both velocity components are zero. At the upper wall the vertical velocity is again zero slip is assumed to occur following a power-law slip equation,

$$\tau_w^* = Bu_w^{*s} \tag{7}$$

where $B \equiv \beta H^n / (kU^{n-s})$ is the (dimensionless) slip number. Finally, the exit plane is taken sufficiently far downstream so that the flow can be assumed fully developed. For the low Reynolds number considered here, we took L_{mesh} =20.

2.1 Fully-developed solutions

The non-dimensionalization introduced above is based on the mean velocity, which implies that there is flow, i.e. Regime I is excluded. Due to the definition of the slip number, the no-slip case, which corresponds to a symmetric velocity profile with respect to the midplane of the channel, is recovered for $B \to \infty$. Obviously, this solution, which involves two symmetric yield points at y_1^* and $y_2^* = 1 - y_1^*$ falls into Regime III. Keeping the Bingham number constant and decreasing the slip number, enhances slip at the upper wall and the velocity becomes asymmetric: the two yield points move towards the upper wall (that is both y_1^* and y_2^* increase) and the size of the plug region ($y_2^* - y_1^*$) increases while its velocity is reduced. This trend continues till a critical slip number, B_c, at which the upper yield point reaches the wall (the dimensionless upper wall shear stress is equal to Bn) signaling the transition from Regime III to Regime II. The general dimensionless solution for $B_c \le B < \infty$ is given by

$$u_x^*(y^*) = \begin{cases} \frac{1}{A_{III}}\left[y_1^{*1/n+1} - (y_1^* - y^*)^{1/n+1} \right], & 0 \le y^* \le y_1^* \\ \frac{y_1^{*1/n+1}}{A_{III}}, & y_1^* \le y^* \le y_2^* \\ u_w^* + \frac{1}{A_{III}}\left[(1-y_2^*)^{1/n+1} - (y^* - y_2^*)^{1/n+1} \right], & y_2^* \le y^* \le 1 \end{cases} \tag{8}$$

where

$$u_w^* = \frac{1}{A_{III}}\left[y_1^{*1/n+1} - (1-y_2^*)^{1/n+1} \right] \tag{9}$$

and

$$A_{III} = y_1^{*1/n+1}\left(1 - \frac{n}{1+2n}y_1^*\right) - \frac{n}{1+2n}(1-y_2^*)^{1/n+2} \tag{10}$$

The positions of the two yield points can be found by solving the following system of equations:

$$(2 - y_1^* - y_2^*)Bn - (y_2^* - y_1^*)Bu_w^{*s} = 0 \tag{11}$$

and

$$(1+1/n)^n (y_2^* - y_1^*) - 2Bn\, A_{III}^n = 0 \tag{12}$$

No-slip case

In the no-slip case ($u_w^* = 0$) Eq. (9) yields

$$y_2^* = 1 - y_1^* \tag{13}$$

which indicates that the flow is symmetric with respect to the midplane of the channel. Substituting into Eq. (10) gives

$$A_{III} = y_1^{*1/n+1}\left(1 - \frac{2n}{1+2n}y_1^*\right) \tag{14}$$

and Eq. (12) then becomes:

$$(1+1/n)^n (1-2y_1^*) - 2Bn\, y_1^{*n+1}\left(1 - \frac{2n}{1+2n}y_1^*\right)^n = 0 \tag{15}$$

Critical value of the slip number

The critical value B_c of the slip number can be found by setting $y_2^* = 1$. Let us denote the corresponding critical values of y_1^* and u_w^* by y_{1c}^* and u_{wc}^*, respectively. From Eq. (11) we get

$$B_c u_{wc}^{*s} = Bn \tag{16}$$

which simply says that the upper wall shear stress is equal to *Bn*. The critical slip velocity is given by

$$u_{wc}^* = \frac{1}{1 - \dfrac{n}{1+2n} y_{1c}^*} \tag{17}$$

and, therefore,

$$B_c = \left(1 - \frac{n}{1+2n} y_{1c}^*\right)^s Bn \tag{18}$$

Finally, from Eq. (12) we get

$$(1+1/n)^n (1 - y_{1c}^*) - 2Bn\, A_{IIIc}^n = 0 \tag{19}$$

or

$$(1+1/n)^n (1 - y_{1c}^*) - 2Bn\, y_{1c}^{*n+1} / u_w^{*n} = 0 \tag{20}$$

which is used to calculate y_{1c}^*. It should be noted that the value of y_{1c}^* is independent of the slip equation parameters. For example, in the Bingham plastic case (*n*=1), y_{1c}^* is a root of

$$Bn\, y_{1c}^{*3} - 3Bn\, y_{1c}^{*2} - 3y_{1c}^* + 3 = 0 \tag{21}$$

while the value of B_c can then be calculated from Eq. (18) for any value of *s*.

Solution in Regime II

If the slip number is further reduced, the yield point keeps moving towards the upper wall and the size of the plug is thus reduced while its velocity increases. Finally, in the limit $B = 0$ (full slip), the velocity profile corresponds to the no-slip solution in a channel of double width (2*H)*, i.e. to the no-slip solution corresponding to the Bingham number

$$Bn' = \frac{\tau_0 (2H)^n}{kU^n} = 2^n Bn \tag{22}$$

Hence, when $0 < B \le B_c$, the flow corresponds to Regime II and the dimensionless velocity is given by

$$u_x^*(y^*) = \begin{cases} \left[y_1^{*1/n+1} - (y_1^* - y^*)^{1/n+1} \right] \Big/ \left[y_1^{*1/n+1} \left(1 - \dfrac{n}{1+2n} y_1^*\right)\right], & 0 \le y^* \le y_1^* \\ u_w^*, & y_1^* < y^* \le 1 \end{cases} \tag{23}$$

where

$$u_w^* = \frac{1}{1 - \dfrac{n}{1+2n} y_1^*} \tag{24}$$

and y_1^* is the root of

$$(1+1/n)^n (1 - y_1^*) - \left(Bn + Bu_w^{*s}\right) y_1^{*n+1} / u_w^{*n} = 0 \tag{25}$$

Substituting Eq. (16) into the above equation yields Eq. (20) for y^*_{1c}. For n=1 (Bingham plastic) and s=1 (Navier slip) Eq. (25) is simplified to

$$Bn\, y_1^{*3} - 3(Bn + B)\, y_1^{*2} - 6 y_1^* + 6 = 0 \qquad (26)$$

Figure 3 illustrates the two flow regimes on the (Bn,B) plane in the case of a Bingham plastic (n=1), separated by the curve $B_c = (1 - y^*_{1c}/3)Bn$, which is slightly below the straight line $B = Bn$. Four representative velocity profiles, obtained taking Bn=1 and assuming Navier slip (s=1), are also shown. Two of them are in Regime III. The first profile corresponds to no-slip at both walls ($B \to \infty$) and it is thus symmetric. As slip at the upper wall is enhanced (e.g., for B=5), symmetry is destroyed and the two yield points move upwards and the maximum velocity decreases. The upper yield point moves faster than the lower one reaching the wall when $B = B_c$. The velocity profile for this critical case is also shown in Fig. 3. Below that number, i.e., in Regime II, the yield point continues moving upwards as slip is increased, but the maximum velocity is now increasing. In the limit of B=0, the maximum velocity is lower than that for $B \to \infty$, since it corresponds to the no-slip flow for a Bingham number equal to $Bn' = 2^n Bn = 2Bn$.

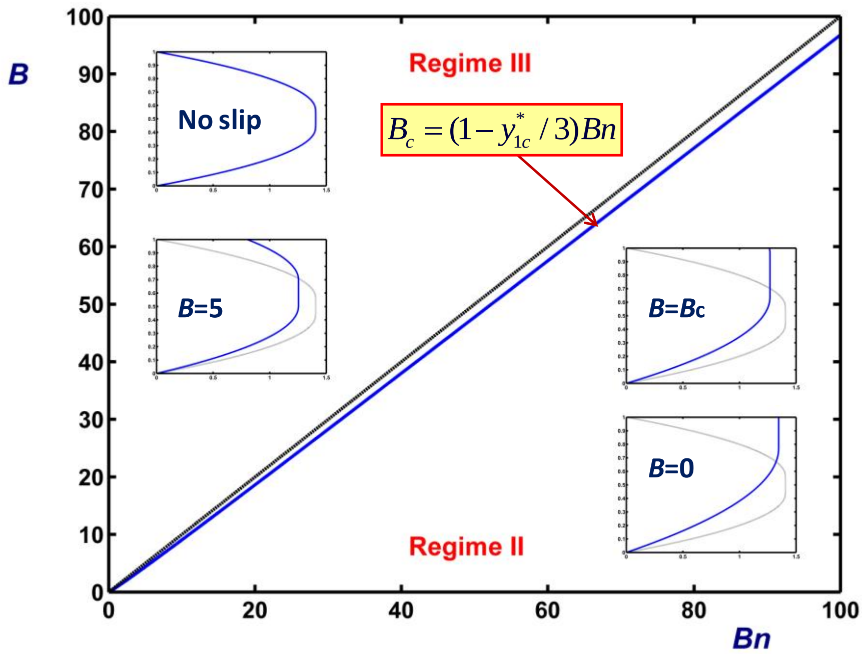

Figure 3: Flow regimes and representative velocity profiles in Bingham plastic (n=1) flow with Navier slip (s=1). The velocity profiles have been obtained for Bn=1 and various slip numbers.

3 PRELIMINARY NUMERICAL RESULTS

The system of the governing equations and the boundary conditions presented in Section 2 was solved numerically using the finite element method (u-v-p formulation) with standard biquadratic basis functions for the two velocity components and bilinear ones for the pressure field. The Galerkin forms of the continuity and the momentum equations were used. The resulting nonlinear system of the discretized equations was solved with a Newton-Raphson iterative scheme with a convergence tolerance equal to 10^{-4}. Results have been obtained first for a Bingham plastic (n=1) with Bn=1 and various values of the slip number B. Figure 4 shows how the velocity component in the flow direction develops downstream attaining the fully developed profile. When B=∞ (no slip), the velocity profiles are symmetric exhibiting a central unyielded region. As slip is increased, asymmetry is enhanced and the unyielded region moves towards upper wall and increases in size. If slip becomes even stronger then Regime II is eventually reached, i.e. the unyielded region reaches the upper wall. This is almost achieved for B=1, as revealed in Fig. 5, where the velocity contours are plotted.

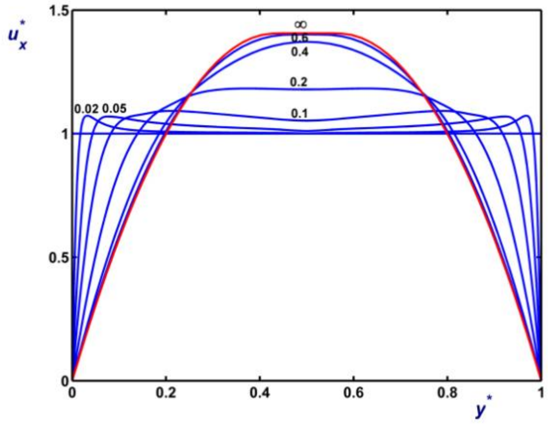

(a)

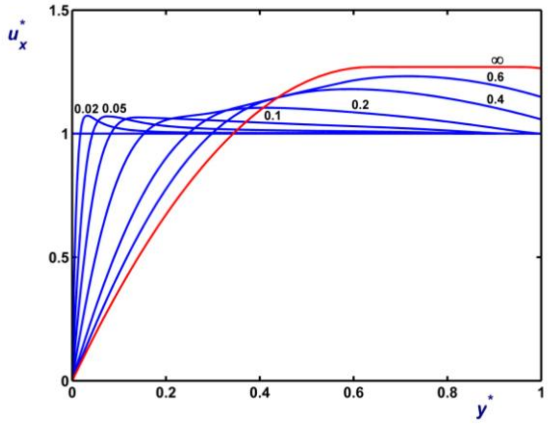

(b)

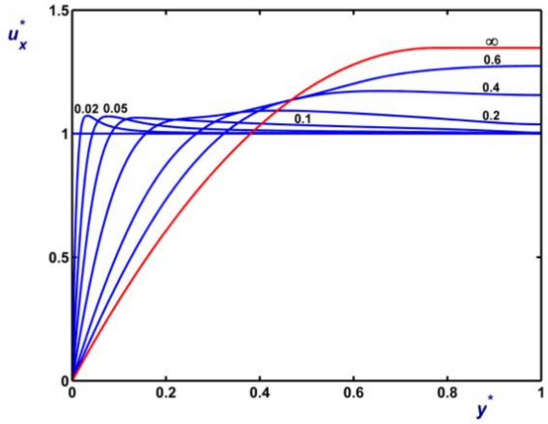

(c)

Figure 4: Development of the velocity in creeping flow (Re=0) of a Bingham plastic (n=1) with Bn=1 and various slip numbers: (a) B=∞ (no-slip); (b) B=1; (c) B=0.01.

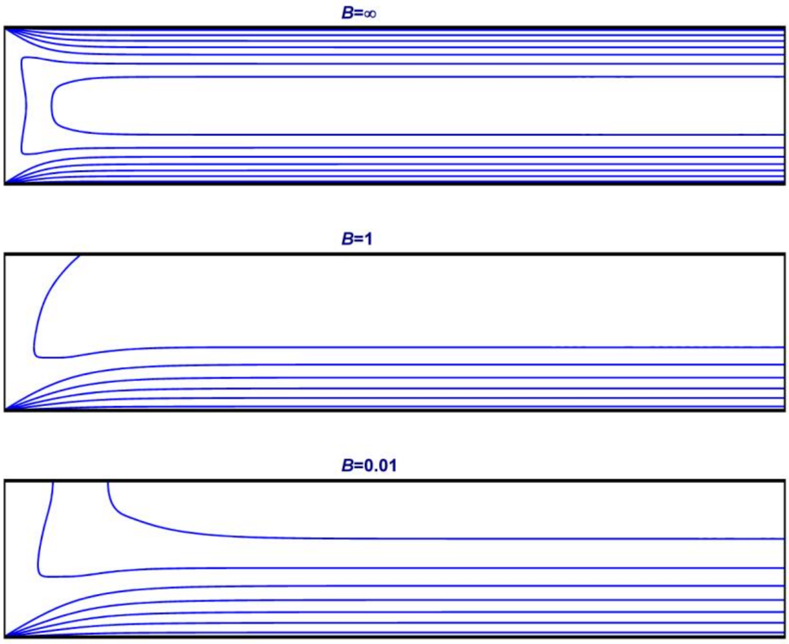

Figure 5: Velocity contours in flow development of a Bingham plastic (n=1) with Bn=1 and B=∞ (no-slip), 1 and 0.01; Re=0, s=1.

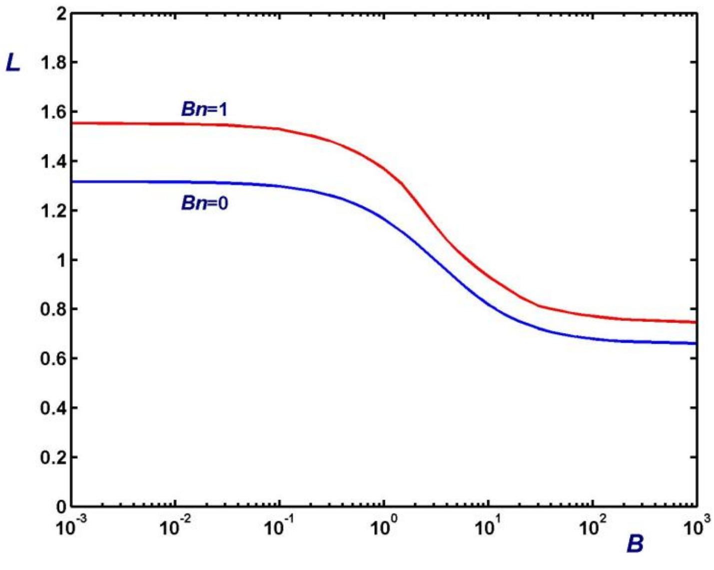

Figure 6: Development length for Bn=0 (Newtonian) and 1 versus the slip number; Re=0, n=1, s=1.

In Fig. 6, the development lengths computed for Bn=0 (Newtonian flow) and 1 are plotted versus the slip number B. Both curves are sigmoidal and the development length increases with the Bingham number. It should be noted that the development length for Newtonian flow (Bn=0) and full slip (i.e. B=0) is two times the development length for the no-slip case (infinite *B*), since it corresponds to the flow development in a channel with no slip and with a gap width equal to 2. This is not the case for Bingham flow; the development length in the full slip case is two times the no-slip development length corresponding not to *Bn*=1 but to *Bn*=2.

4 CONCLUSIONS

We have solved numerically the entry flow of a Herschel-Bulkley fluid in a channel with asymmetric wall slip using finite elements and a regularized constitutive equation. We have considered in particular the case where there is slip only on the upper wall, identified the different flow regimes, and derived the fully-developed solutions. The effects of the Bingham and slip numbers on the development of the velocity and the development length have been discussed.

REFERENCES

[1] U. Yilmazer, D.M. Kalyon, Slip effects in capillary and parallel disk torsional flows of highly filled suspensions. *Journal of Rheology*, **33**, 1197-1212, 1989.

[2] H.A. Barnes, A review of the slip (wall depletion) of polymer solutions, emulsions and particle suspensions in viscometers: Its cause, character, and cure. *Journal of Non-Newtonian Fluid Mechanics*, **56**, 221-251, 1995.

[3] P. Ballesta, G. Petekidis, L. Isa, W.C.K. Poon, R. Besseling, Wall slip and flow of concentrated hard-sphere colloidal suspensions. *Journal of Rheology*, **56**, 1005-1037, 2012.

[4] M.M. Denn, Extrusion instabilities and wall slip. *Annual Reviews in Fluid Mechanics*, **33**, 265-287, 2001.

[5] D.M. Kalyon, Apparent slip and viscoplasticity of concentrated suspensions, *Journal of Rheology*, **49**, 621-640, 2005.

[6] C.L.M.H. Navier, Sur les lois du mouvement des fluides. Mémoires de l'Academie des Sciences de l'Institute de France, **6**, 389-440, 1827.

[7] A.L. Vayssade, C. Lee, E. Terriac, F. Monti, M. Cloitre, P. Tabeling, Dynamical role of slip heterogeneities in confined flows. *Physics Reviews*, **89**, 052309, 2014.

[8] T.C. Papanastasiou, Flows of materials with yield, *Journal of Rheology*, **31**, 385-404, 1987.

[9] R. Shah, A. London, *Laminar flow forced convection in ducts: a source book for compact heat exchanger analytical data*, Academic Press, 1978.